Cellular signalling effects in high precision radiotherapy

McMahon, S. J., McGarry, C. K., Butterworth, K. T., Jain, S., O'Sullivan, J. M., Hounsell, A. R., & Prise, K. M. (2015). Cellular signalling effects in high precision radiotherapy. *Physics in Medicine and Biology*, *60*(11), 4551-4564. https://doi.org/10.1088/0031-9155/60/11/4551

Published in:
Physics in Medicine and Biology

Document Version:
Publisher's PDF, also known as Version of record

Cellular signalling effects in high precision radiotherapy

2015 Phys. Med. Biol. 60 4551

(http://iopscience.iop.org/0031-9155/60/11/4551)

OPEN ACCESS
IOP Publishing | Institute of Physics and Engineering in Medicine Physics in Medicine & Biology
Phys. Med. Biol. **60** (2015) 4551–4564 doi:10.1088/0031-9155/60/11/4551

Cellular signalling effects in high precision radiotherapy

Stephen J McMahon[1], Conor K McGarry[1,2], Karl T Butterworth[1], Suneil Jain[1,3], Joe M O'Sullivan[1,3], Alan R Hounsell[1,2] and Kevin M Prise[1]

[1] Centre for Cancer Research and Cell Biology, Queen's University Belfast, Lisburn Road, Belfast BT9 7AE, UK
[2] Radiotherapy Physics, Northern Ireland Cancer Centre, Belfast Health and Social Care Trust, Lisburn Road, Belfast, BT9 7AB, UK
[3] Clinical Oncology, Northern Ireland Cancer Centre, Belfast Health and Social Care Trust, Lisburn Road, Belfast, BT9 7AB, UK

E-mail: stephen.mcmahon@qub.ac.uk

Received 30 January 2015, revised 24 March 2015
Accepted for publication 9 April 2015
Published 20 May 2015

Abstract

Radiotherapy is commonly planned on the basis of physical dose received by the tumour and surrounding normal tissue, with margins added to address the possibility of geometric miss. However, recent experimental evidence suggests that intercellular signalling results in a given cell's survival also depending on the dose received by neighbouring cells. A model of radiation-induced cell killing and signalling was used to analyse how this effect depends on dose and margin choices. Effective Uniform Doses were calculated for model tumours in both idealised cases with no delivery uncertainty and more realistic cases incorporating geometric uncertainty. In highly conformal irradiation, a lack of signalling from outside the target leads to reduced target cell killing, equivalent to under-dosing by up to 10% compared to large uniform fields. This effect is significantly reduced when higher doses per fraction are considered, both increasing the level of cell killing and reducing margin sensitivity. These effects may limit the achievable biological precision of techniques such as stereotactic radiotherapy even in the absence of geometric uncertainties, although it is predicted that larger fraction sizes reduce the relative contribution of cell signalling driven effects. These observations may contribute to understanding the efficacy of hypo-fractionated radiotherapy.

Keywords: conformal radiotherapy, margins, radiobiology, intercellular signalling, mathematical modelling

(Some figures may appear in colour only in the online journal)

1. Introduction

Although advances in radiotherapy delivery such as Intensity Modulated Radiotherapy (IMRT) and Volumetric Modulated Arc Therapy (VMAT) offer significant improvements in dose conformality, exposure of normal tissue remains a limiting factor in many cases.

One major challenge in this area is uncertainty in treatment set-up and delivery, where patient motion may lead to treatment fields no longer being aligned with target structures, an effect known as geometric miss. This can cause significant under- and over-dosing of tumour and organs at risk. To account for geometric miss in clinical scenarios, once the Clinical Target Volume (CTV) has been delineated, an additional margin is added to give the Planning Target Volume (PTV) (ICRU 1993). As this necessarily requires additional exposure of normal tissues, there is considerable interest in minimising geometric uncertainties and determining margin recipes to accurately compensate for them (Van Herk *et al* 2000, van Herk 2004, Herschtal *et al* 2013, Selvaraj *et al* 2013). Reductions in margins are not without risk, however, as under-dosing of tumours may significantly impact upon local control.

Even if geometric issues can be fully addressed, there may remain motivation for irradiating targets larger than the CTV. This is due to non-targeted radiobiological effects driven by intercellular signalling—commonly known as bystander effects (Prise and O'Sullivan 2009). While typically associated with low dose exposures, recent results have shown large contributions from communication between cells exposed to high doses which remain in contact for extended periods (Suchowerska *et al* 2005, Mackonis *et al* 2007, Butterworth *et al* 2011, Butterworth *et al* 2010), with reports of bystander cell killing of more than 50% and saturation doses greater than 4 Gy. This has been further supported by evidence of significant out-of-field effects in *in vivo* systems (Mancuso *et al* 2008, Mancuso *et al* 2013).

Recent mathematical analysis has suggested that intercellular communication may play a significant role in cell death even in populations exposed to doses up to several Gray (Ebert *et al* 2010, Blyth and Sykes 2011, McMahon *et al* 2012, McMahon *et al* 2013a, Balderson and Kirkby 2014). This is potentially very important for radiotherapy planning, as any dependence of in-target cell killing on out-of-field dose would conflict with the goal of minimising exposure of healthy tissue. A recent study (McMahon *et al* 2013b) investigated prostate radiotherapy plans incorporating intercellular signalling, finding small but consistent impacts on predicted tumour killing compared to plans considering physical dose alone (equivalent to approximately 5% target under-dosing).

However, that work did not investigate the impact of either fractionation schedule or margin prescription, both of which may significantly impact on the contribution of signalling effects. These factors are particularly important in current radiotherapy practice, as Stereotactic Ablative Radiotherapy (SABR) has emerged as a treatment option for localised cancers, delivering treatments with large fraction sizes and extremely small margins of 3–5 mm or less, with interest in further reductions through image guided radiotherapy techniques. These approaches have shown excellent clinical results, leading to considerable interest in their underlying biology (Sheu *et al* 2013, Brown *et al* 2014, Tree *et al* 2014), although there has been a large variation in dose fractionation regimes utilised in clinical studies.

This work investigates the impact of margin and fractionation choice on tumour cell killing in light of intercellular signalling, both in an idealised scenario as well as one incorporating geometric uncertainties.

2. Methods

2.1. Treatment scenario and dose distributions

As in previous radiotherapy margin studies (Van Herk *et al* 2000, van Herk 2004, Selvaraj *et al* 2013), the irradiation of spherical CTVs was modelled. Dose deliveries are prescribed to a PTV, which is defined as the CTV plus a uniform margin. These volumes are embedded in a larger tissue volume, sized such that the PTV has a margin of at least 30 mm in all directions. For computational purposes, this volume is divided into 1 mm^3 voxels.

Spherically symmetric conformal dose distributions were modelled, with radial dose distributions of $D(r) = \frac{D_0}{1 + e^{a(r-(r_0+d))}}$, where D_0 is the prescription dose, r is the distance from the centre of the CTV, and r_0 is the total PTV radius. This gives a sigmoidal dose distribution centred on the target, with 50% dose delivered at a distance of d from the PTV edge. While idealised, these dose distributions are comparable to those which can be delivered clinically through techniques such as VMAT (Selvaraj *et al* 2013). An illustration of this dose distribution is shown in figure 1.

The distance d is set to 5 mm, and the steepness of the dose distribution (characterised by a) is set such that the edge of the PTV sees 95% of the prescription dose, which leads to an 80% to 20% penumbral width of 4.8 mm.

2.2. Intercellular signalling model

Survival incorporating intercellular signalling is investigated using previously published models (McMahon *et al* 2012, McMahon *et al* 2013a, 2013b), summarised briefly below.

Within each voxel, cells are exposed to a uniform dose. This causes direct damage (proportional to dose) and induces the secretion of potentially damaging signals. These signals are produced by cells for a time proportional to the physical dose they receive and are assumed to be unstable, being depleted in a simple exponential decay with coefficient λ. In uniformly irradiated populations, this leads to a signal which builds towards an equilibrium concentration before decaying away as cells cease signalling.

Above a certain signal threshold, cells are assumed to suffer the induction of signalling-induced damage at a constant rate. This gives a probability of $P_B = 1 - e^{-\kappa\tau}$ for cells experiencing signalling-induced damage, where κ is a response coefficient and τ is the time for which cells are exposed to an above-threshold signal. The level of damage caused is characteristic of the cell-line. Survival is determined from a cumulative damage model. Briefly, both direct radiation-induced and indirect signalling-induced damage translate into a number of microscopic damage events ("hits") within each cell, taken to be Poisson distributed around mean values determined by dose and the time to which cells are exposed to an above-threshold level of signal. This can then potentially lead to cell death either immediately or through mitotic catastrophe at the next cell division, with probabilities that depend on the level of damage within each cell. By calculating average damage levels within each voxel, predictions of cell damage can thus be made. Further detail can be found in previous publications (Partridge 2008, McMahon *et al* 2012).

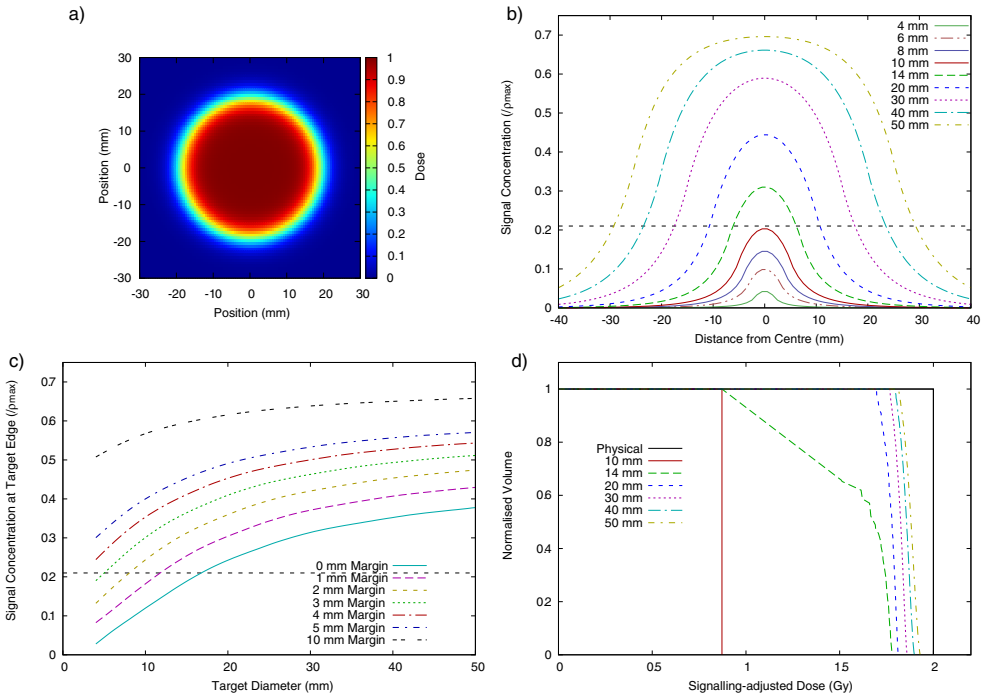

Figure 1. (a) Dose distribution through central plane of 20 mm irradiated sphere, exposed with a 5 mm margin and $d = 5$ mm. (b) Signal concentration around uniformly irradiated spheres of different diameters, irradiated with zero margin. Horizontal line indicates the response threshold. (c) Signal concentration at the edge of volumes of different sizes, exposed with a range of margins. (d) DVHs for a series of target sizes, exposed with zero margins. A perfectly conformal delivery of 2 Gy (solid line) leads to a variety of different signalling-adjusted dose distributions (dashed lines) depending on target size.

In regions which are exposed to modulated fields, signals homogeneously diffuse between voxels. This diffusion leads to shifts in the levels of signalling, and thus cell killing, compared to uniform irradiations. Signal production and diffusion was modelled in a series of timesteps until all cells ceased signalling and the maximum concentration fell below the response threshold, allowing for total exposure times to be calculated for each voxel. These were used to calculate the probability of signalling-induced damage for cells within each voxel, which in turn were used to calculate survival probabilities as outlined above. Input parameters for this study were based on those derived for DU-145 prostate cancer cells (McMahon *et al* 2013a), giving LQ parameters of $\alpha = 0.15$ and $\alpha/\beta = 3$ for uniform exposures, as seen experimentally (Butterworth *et al* 2012).

Signal production rates, ν, were estimated as a value of $\nu = 0.05\rho_{\max}$ min^{-1} per voxel, where $\rho_{\max}$ is the maximum signal concentration. This is sufficient to drive a response if over 10% of the population has been exposed, as observed experimentally (Butterworth *et al* 2012). While actual *in vitro* or *in vivo* signal concentrations are poorly quantified, in this model survival only depends on the relative values of the maximum signal, production rate and response threshold. Thus, all signal concentrations were modelled in units of the maximum concentration, using a threshold from previous work (McMahon *et al* 2013a).

The rate of signal diffusion *in vivo* remains poorly characterised. Here, diffusion is characterised in terms of the equilibrium range, given by $r = \sqrt{D/\lambda}$, where D is the diffusion coefficient. In the examples below, this range is taken as 10 mm, an estimate based on reported measurements of *in vivo* bystander effects (Mancuso *et al* 2013). In the cases considered here, predictions would remain unchanged if both this range and physical dimensions are scaled by the same factor.

An analysis of the model's sensitivity to changes in signal range and production parameters is presented in appendix A.

In this analysis, dose delivery is assumed to occur instantaneously, rather than being built up over a period of time through multiple fields as is the case in clinical treatment. While a simplification, experimental evidence suggests that signalling effects are not significantly affected if cells are irradiated using a single acute exposure or a longer exposure delivered using techniques such as IMRT or VMAT (McGarry *et al* 2012). Additionally, signal kinetics (McMahon *et al* 2013a) suggest that provided the total treatment duration is smaller than the total signal production time (on the order of 1 h Gy^{-1} in DU145 cells), the impact of dose rate would be small.

2.3. Dose Quantification

As the model used in this work predicts a survival level for each individual voxel, 'signalling-adjusted' doses were used for comparisons between model predictions and physical plans (McMahon *et al* 2013b). For a voxel with modelled survival S_i, the signalling-adjusted dose D_S is defined as the dose which would yield the same survival in the limiting case of a large uniform exposure, that is $e^{-\alpha D_S - \beta D_S 2} = S_i$, where α and β are determined from the model's predictions for uniform exposures as noted above.

For comparison between different treatments, CTV Equivalent Uniform Doses (EUDs) were calculated, given as $e^{-(\alpha \mathrm{EUD} + \beta \mathrm{EUD}^2)} = \sum v_i e^{-(\alpha D_i + \beta D_i^2)}$, where v_i is the fraction of the volume exposed to the dose D_i, where D_i can be defined either as the physical dose seen by the voxel or the signalling-adjusted dose predicted by the model, to compare between physical and model predictions.

2.4. Patient data

An illustrative prostate radiotherapy case was analysed to show these effects in a realistic geometry. An initial series of VMAT plans were created with symmetric prostate margins of 0, 3, 5, 10 or 15 mm with a prescription dose of 8 Gy per fraction over 5 fractions. These plans were created using the Eclipse treatment planning system version 11.0.42 (Varian Medical Systems, Palo Alto, CA) for delivery on a Varian Truebeam linear accelerator using a single arc (30 degree collimator rotation) with a 10 MV flattening filter free (FFF) photon beam of dose rate 2400 MU min^{-1}. Plans were normalised so that 98% of the PTV was irradiated to 98% of the prescription dose. An upper limit of 125% was placed on the PTV and was achieved for all margins except for 15 mm. Doses to the urethra, rectum and bladder were minimised as much as possible but the priority was placed on coverage of the PTV. The fraction sizes were scaled to between 2 and 10 Gy per fraction for fractionation analysis.

2.5. Target displacement

One of the primary motivations for treatment margins is geometric errors. To investigate their impact on signalling, motion was incorporated in a similar fashion to Selvaraj (Selvaraj *et al* 2013).

Multi-fraction treatment courses were modelled using a Monte Carlo approach. 100 independent treatment courses were generated for each dose and margin combination to sample possible motion impacts. Within each treatment course, individual fractions were calculated independently, with the position of the CTV shifted to represent both systematic uncertainties (a common offset across all fractions in a given treatment course) and random errors (an additional, independent shift in each fraction). These errors were generated by sampling 3D Gaussian distributions.

The overall impact of motion was quantified by accumulating cell killing across a treatment course, assuming no signal persisted between fractions. This was converted into an EUD per fraction value for ease of comparison. Repopulation was neglected in this analysis, as it would be expected to only provide a constant offset.

3. Results

3.1. Target size and signalling-driven effects

Figure 1(b) illustrates the equilibrium signal concentration for targets of various diameters exposed to conformal irradiation with zero margin. Peak concentrations are dependent on target size, with significant fall-off at target edges. For very small volumes (<10 mm) the peak concentration is below the response threshold, preventing any signalling-induced cell killing. Figure 1(c) illustrates this, showing the signal concentration at the edge of the CTV. For irradiations with no margin, signals do not exceed the response threshold until diameters of at least 18 mm. This can lead to significant heterogeneity in cell-killing in these targets, despite uniform physical doses. This effect is reduced by adding margins, leading to higher signal concentrations and better uniformity across the CTV.

Figure 1(d) presents the signalling-adjusted dose volume histograms (DVHs) for such targets exposed to uniform doses of 2 Gy. Despite identical physical DVHs, significant variations occur in modelled cell-killing and thus signalling-adjusted doses. As reported elsewhere (McMahon *et al* 2012), at these doses intercellular communication drives a large portion of cell killing, so a dramatic reduction in effect is seen in the smallest targets which experience no signalling-driven death. This is mitigated in larger targets due to increasing signalling, but even in larger targets there is a degree of heterogeneity (∼5%) and a loss in overall effect (∼10%) due to reduced signalling compared to uniform doses.

Figure 2 summarises the potential impact of these signalling-driven effects on the CTV EUD following 2 Gy dose delivery to targets of varying sizes and margin prescriptions. For the smallest targets (4 mm) there is a reduction equivalent to nearly a 20% under-dosing of the target volume due to the lack of signalling-driven effects, although even a 1 mm margin significantly abrogated this effect. The scale of this effect reduces gradually with increasing target size, with a 5% reduction in EUD for a 5 cm target irradiated with no additional margins.

These results suggest that even where therapy could be delivered without geometric errors, there is still a non-trivial benefit of some treatment margin, due to increased cell-killing by signalling from non-tumour cells.

3.2. Varying dose per fraction

Due to normal tissue toxicities, margins are particularly significant in hypo-fractionated treatments. However, signalling-driven effects are known to saturate at higher doses (Butterworth *et al* 2011, Butterworth *et al* 2012), suggesting they may have a reduced importance for larger

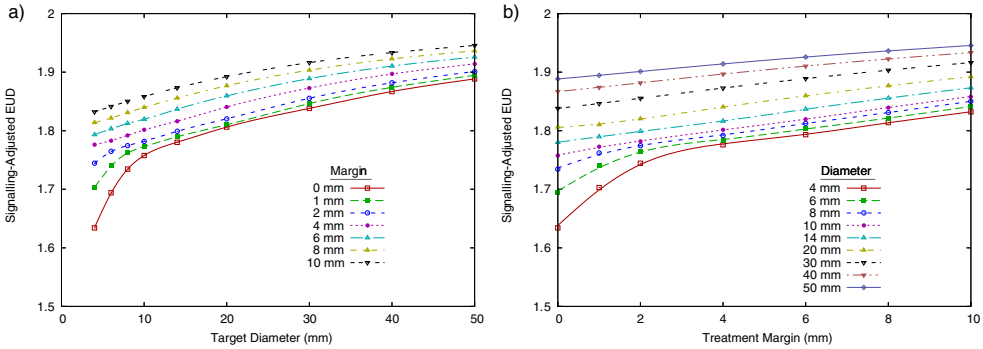

Figure 2. Effects of varying target diameter and margin on signalling-adjusted EUD, for irradiation of spherical targets to 2 Gy. (a) Effect of varying target diameter for different margin prescriptions. (b) Effect of varying margins for different target diameters.

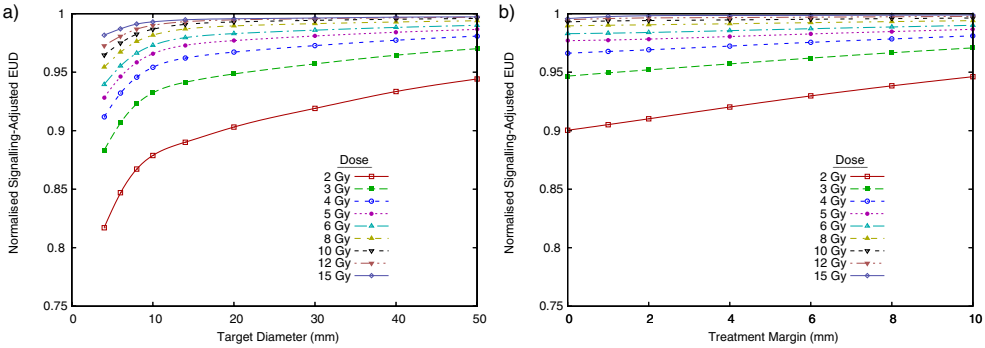

Figure 3. Effects of target diameter and margin on normalised signalling-adjusted EUD, at varying physical doses. (a) Effect of varying target diameter with no margins at different doses. (b) Effect of varying treatment margin on a 20 mm target volume, at different doses.

fractions. Figure 3 presents normalised signalling-adjusted EUDs for varying fraction sizes (i.e. signalling-adjusted EUD divided by the physical plan EUD).

While similar trends are seen, the scale of the effect is dramatically reduced at higher doses. For zero margin cases, 4 Gy fractions see roughly half the reduction in cell killing at 2 Gy, with the effect reduced to a few percent at the highest doses. This has the additional effect of reducing the sensitivity to margins. While 10 mm margins increased EUDs for 20 mm targets by roughly 5% at 2 Gy, this is on the order of 1% at 4 Gy.

3.3. Patient Data

Figure 4 presents the impact of these effects in a clinical prostate radiotherapy plan, planned with zero CTV margin, and a volume equivalent to a target diameter of 48 mm. When compared to physical dose (top), incorporating signalling-driven effects leads to a significant drop in target EUD for 2 Gy fractions (7%, middle), with nearly 20% of the 2 Gy target volume now falling below the prescription dose. However, as fraction size is increased this effect is diminished, and at 8 Gy fractions little impact is seen (bottom, 1%). These differences are highlighted by dose difference plots (right middle & bottom) which show the change in

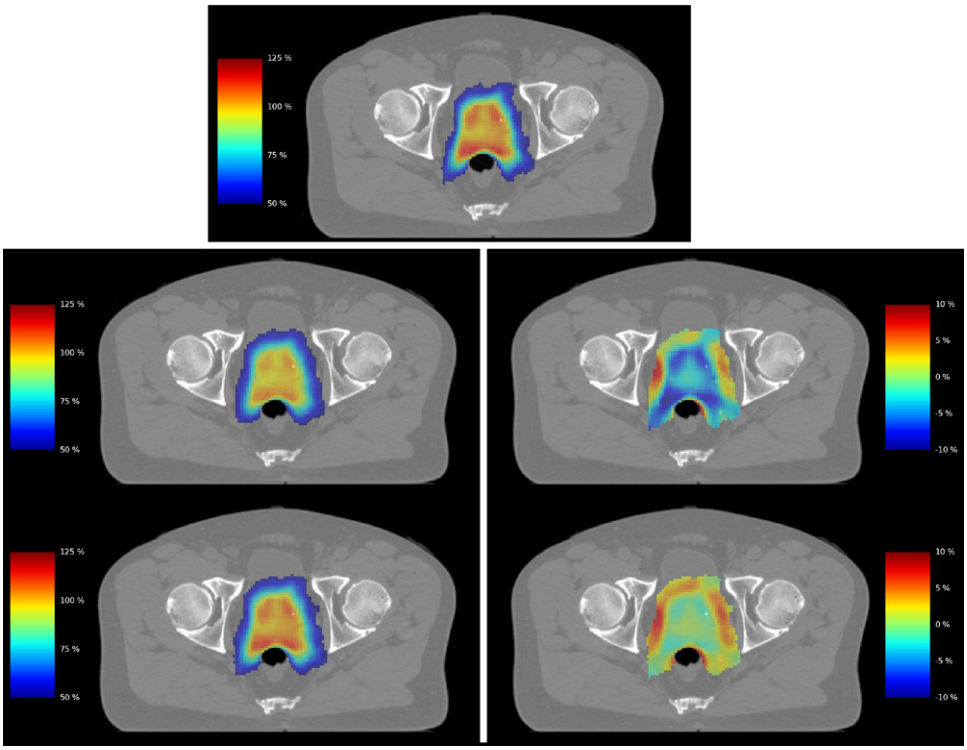

Figure 4. Illustration of reduced signalling in clinical external beam radiotherapy plan. In this VMAT plan, a given physical dose distribution (top) is converted into signalling-adjusted dose for doses of 2 (middle) or 8 (bottom) Gy per fraction. Treatments are illustrated either as effective dose maps (left) or dose difference maps (right) for voxels which see greater than 50% of the prescription dose. A significant drop in target dose is seen compared to the physical case at 2 Gy, while good correspondence is seen at 8 Gy per fraction.

effective dose between signalling-adjusted and physical doses for high-dose voxels (those seeing >50% of the prescription dose). Outside the target, both fraction sizes see significant increases in cell killing in the lower-dose region immediately surrounding the target. More detailed discussion of signalling effects in low-dose regions can be found in previous work (McMahon *et al* 2013b).

Signalling-adjusted EUD analysis was carried out for each of these treatment plans, and is presented in figure 5, normalised to prescription dose as in figure 3. While comparisons between different margin and dosing selections are more difficult due to the increased field complexity needed to deliver treatments with the very smallest margins, the key observations from the simpler model—that the irradiation of tissue outside the target volume or the use of higher doses increases biological effectiveness—remain even in this more complex scenario.

3.4. Tumour motion and fraction size

Figure 6 illustrates the impact of motion in this model. Treatments with an EQD2 of 74 Gy were modelled, either as 37×2 Gy fractions, or fewer fractions (illustrated on the upper x axis) at higher dose per fraction, for a 20 mm diameter CTV with systematic and random uncertainties of 3 mm standard deviation.

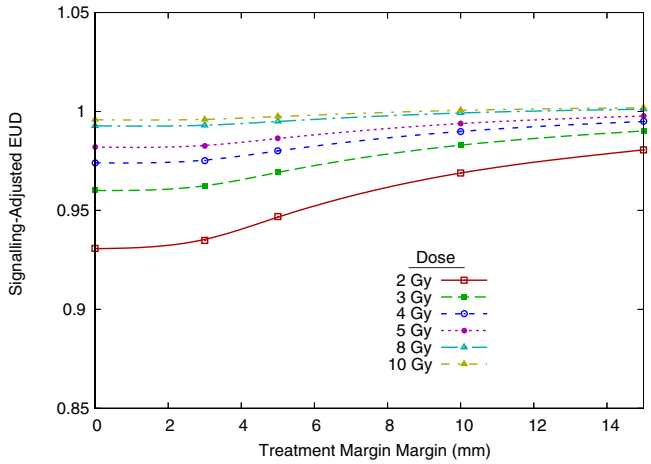

Figure 5. Effects of varying margin and dose per fraction on normalised signalling-adjusted EUD for a patient geometry. As in the idealised case, increases in both fraction size and margin prescription lead to predicted increases in EUD.

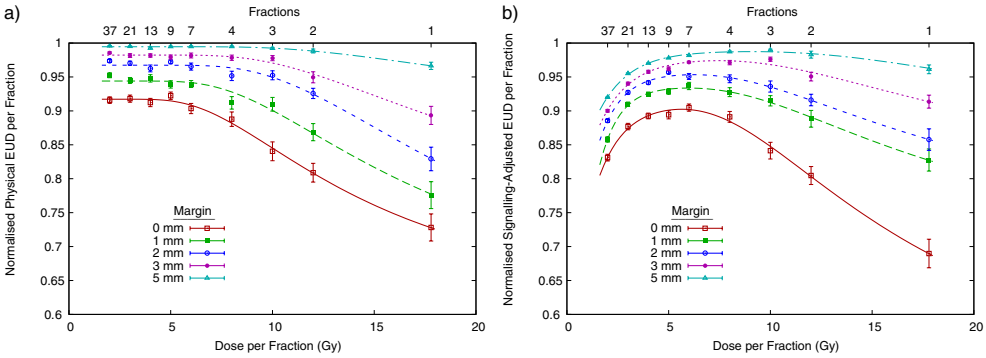

Figure 6. Effects of incorporating physical motion into treatment plans. EUDs were calculated for a 20 mm target with 3 mm geometric uncertainties. (a) Impact of motion on EUD for the physical dose plan, showing reduced efficacy for fewer fractions due to geometric miss. (b) Impact of motion on signalling-adjusted EUD. Large numbers of small fractions see a reduction in effectiveness due to relatively smaller signalling-driven effects. Error bars are standard errors from 100 simulations.

For physical dose distributions alone (figure 6(a)), these results are comparable to previous publications (Selvaraj *et al* 2013). Geometric uncertainties have a greater impact in hypo-fractionated treatments, due to larger risks of geometric miss and sub-sequent under-dosing. Margins reduce this effect, but the overall trend remains similar. However, as shown in figure 6(b), signalling effects significantly complicate this analysis.

Because the risk of geometric miss now competes with the loss of signalling-driven killing, normalised EUD no longer strictly decreases with increasing fraction size. Instead, there is a broad maximum at moderate fraction number (5–10, for DU-145 cells), which offers a balance between mitigating signalling effects and offsetting the risk of geometric miss.

4. Discussion

Radiotherapy optimised according to physical dose is a successful cancer treatment, with technological advances driving significant improvements in patient outcome. However, there is increasing interest in biological optimisation, incorporating not only geometry but also the underlying tumour and normal tissue biology. In this approach, signalling-driven cell killing is a complex confounding factor, as it requires an incorporation of spatially-dependent biological information rather than the voxel-by-voxel optimisation currently performed.

This study makes several predictions which may impact on planning decisions. One of the most important is that cell killing within the target depends, in part, on sufficient signalling from irradiation of surrounding normal tissue. While particularly significant for very small targets, even in large tumours irradiation of surrounding normal tissue raises the maximum signal level and slows its fall-off, leading to increased tumour kill. This suggests that margins play both a geometric and biological role, and that these "biological margins" may act as a lower bound for conformality, even when geometric uncertainties are minimised.

Larger doses per fraction serve to minimise these effects as they are less dependent on signalling from outside the target volume to kill cells. However, increases in fraction size must be weighed against the risk of geometric miss due to reduced fraction number. As illustrated in figure 6(b), this leads to reduced efficacy of both very small and very large fractions, with an optimum fraction size for these DU-145 prostate cancer cells between 5 and 8 Gy. These fraction sizes have been utilised in several prostate SBRT studies (King *et al* 2012, Loblaw *et al* 2013).

These effects may contribute to the apparent biological effectiveness of hypo-fractionated treatments (Onishi *et al* 2004, Malmström *et al* 2012, McBride *et al* 2012), in two ways. The first is by delivering higher EUDs at larger fraction sizes for otherwise identical treatments than would be estimated from uniform α/β values. The second is the reduced dependence on margins in larger fractions, which may contribute to the success of stereotactic treatments with very small margins.

Clinical validation of these effects is a challenging prospect. While this model suggests a degree of divergence from the traditionally assumed linear-quadratic model, the divergence is relatively small (leading to an effective shift on the order of 10% in EUD). This may be masked by an apparent reduction in the α/β ratio of a similar magnitude, which is significantly less than the uncertainty in parameters determined from clinical data (Tree *et al* 2014).

Some evidence suggests that smaller fractions are more sensitive to margin prescriptions. Several groups have reported losses in prostate cancer tumour control with tighter margins or more conformal radiotherapy delivery (Engels *et al* 2009, Heemsbergen *et al* 2013), suggesting that margins greater than that estimated from geometric parameters may be needed to maintain tumour control. By contrast, in hypo-fractionated treatments, extremely small margins have been successfully used on targets in a variety of sites, despite the expected increase in sensitivity to geometric miss. These data, coupled with interest in highly modulated therapies such as dose painting (Bentzen 2005) suggests that there is merit in further investigating these effects, as there remains uncertainty about the distribution and causes of recurrence following these therapies.

There is also considerable uncertainty in many model parameters. While the sensitivity analysis presented in appendix A suggests that overall trends are consistent across a range of parameter values, quantitative clinical application will require more robust parameter validation, as well as an understanding of the effects of communication between different cell types and the impact of micro-environmental factors such as hypoxia.

Notably, the *in vivo* range of these signals remain uncertain, due to the few studies of highly heterogeneous dose distributions in humans or animals. Range quantification is further complicated due to heterogeneous signal diffusion behaviours, both spatially (due to differences in vascularisation or boundaries between organs) and temporally (as radiotherapy can have significant impacts on vasculature throughout treatment).

The use of small animal radiotherapy platforms (Verhaegen *et al* 2011) may provide valuable insight in this area, through *in vivo* delivery of both clinically-relevant dose distributions and highly heterogeneous doses which could not be delivered clinically but may be relevant to probing cellular communication effects.

5. Conclusion

Incorporating intercellular signalling into analysis of margin effects in radiotherapy suggests there may be a limit to achievable biological conformality even where geometric uncertainties can be eliminated. These effects may be mitigated through the adoption of more biologically optimised planning techniques or the use of larger fraction sizes to minimise the contribution of signalling effects. Further *in vivo* data are needed to verify the potential clinical impacts of these effects.

Acknowledgments

This work was supported by grants from Cancer Research United Kingdom (Grant no. C1513/A707 to KMP, and C212/A11342 for SJM and ARH). SJM is currently supported by funding from the European Community's Seventh Framework Programme FP7-PEOPLE-2013-IOF (Project no. 623630).

Appendix A. Sensitivity analysis

While the values chosen for parameters in this work have been informed by *in vitro* and *in vivo* data, there remains considerable uncertainty, both due to varying cell types and differences between experimental and clinical scenarios. To address this, the sensitivity of the model's EUD predictions to variations in signal range, production rate and decay coefficient has been assessed. In all cases, 2 Gy physical dose exposures with no margin were modelled, for target with diameters of 10 mm, 20 mm and 30 mm. Figure A1 presents the results of varying these parameters, with all other parameters fixed at the value given in the main text.

Panels a and b show the impact of signal range. Panel a shows that the EUD falls as a function of increasing signal range, compared to a large uniform exposure. Greater signal ranges imply more rapid signal diffusion, which both decreases the maximum signal for a given target of finite size and increases the rate at which signal escapes from the target as cells cease signalling. For zero signal ranges, these models return to the same value as local physical dose models (the maximum EUD is slightly less than 2 Gy due to physical dose heterogeneity across the target). As noted in the main text, the model's predictions are largely unchanged if signal range and physical dimensions are scaled equally. This is illustrated in panel b, which shows that the reduction in EUD is approximately equal when the ratio of signal range to target diameter is equal.

Panel c shows the dependence of signalling-adjusted EUD on signal production rate. This is a relatively simple dependence, where at very low production rates (roughly equal to or less

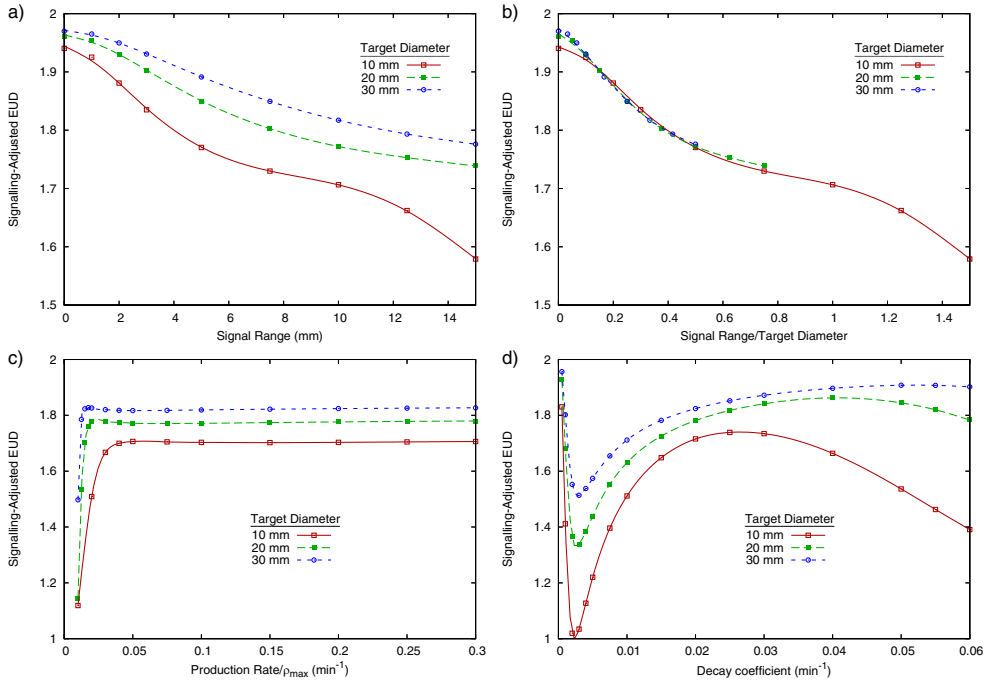

Figure A1. Model predictions for signalling-adjusted EUD, based on variation of signal range (top), production rate (bottom left) or signal decay (bottom right). Signalling-adjusted EUD falls with increasing range (a), with a rate which depends on the relative length scales of target and range (b). Signalling-adjusted EUD shows a relatively build-up and saturation with production rate (c). A more complex dependency is seen with signal decay (d), which is discussed in the text below. Values of 10 mm, 0.05 min^{-1} and 0.019 min^{-1} were used in the main text for signal range, production rate and decay coefficient, respectively.

than the decay rate, λ) there is a significant reduction in signalling-adjusted EUD, as signal concentrations remain below those which can drive damaging responses. This effect saturates rapidly with increasing signal production, and above the $0.05\rho_{\text{max}}$ min^{-1} rate used in this work, little effect is observed as full signalling is seen across the target following radiation exposure.

Panel d shows the more complex dependency on the signal decay coefficient, reflecting the interplay between several characteristics. As seen in c, where the decay coefficient is large compared to the production rate, cell killing and thus signalling-adjusted EUD fall as the maximum signal concentration is reduced by rapid decay, requiring larger irradiated volumes to generate an above-threshold response. Indeed, when $\nu/\lambda < \rho_t$, decay is sufficient to ensure that no signalling-driven effects can be triggered even in a uniformly irradiated volume. For lower decay coefficients, a reduction in signalling-adjusted EUD is also seen, as the effect of signal diffusion is increased compared to uniform exposures which would not be subject to such diffusion. Notably, at extremely low decay coefficients, this trend reverses again, with a sharp increase in signalling-adjusted EUD. This effect is driven by signals becoming so long-lived that they remain above threshold for extremely long periods, even with diffusion of signal throughout the modelled volume. These parameters are relatively balanced across a broad maximum in the range 0.01 to 0.05 min^{-1} (characteristic decay times on the order of 20 to 100 min), around the experimentally determined decay rate of 0.019 min^{-1}.

While considerable variation in EUD is seen with many of these parameters, the overall trends are relatively stable, particularly in the region of the parameters used within this work. It should also be noted that many choices of extreme parameter values are not compatible with biological knowledge. For example, if decay coefficients were near zero, then very high levels of cell killing would be expected even for very low doses, which is not compatible with established linear-quadratic responses.

References

Balderson M J and Kirkby C 2014 Potential implications on TCP for external beam prostate cancer treatment when considering the bystander effect in partial exposure scenarios *Int. J. Radiat. Biol.* **90** 133–41

Bentzen S M 2005 Theragnostic imaging for radiation oncology: dose-painting by numbers *Lancet Oncol.* **6** 112–7

Blyth B J and Sykes P J 2011 Radiation-induced bystander effects: what are they, and how relevant are they to human radiation exposures? *Radiat. Res.* **176** 139–57

Brown J M, Carlson D J and Brenner D J 2014 The tumor radiobiology of SRS and SBRT: are more than the 5 Rs involved? *Int. J. Radiat. Oncol. Biol. Phys.* **88** 254–62

Butterworth K T, McGarry C K, O'Sullivan J M, Hounsell A R and Prise K M 2010 A study of the biological effects of modulated 6 MV radiation fields *Phys. Med. Biol.* **55** 1607–18

Butterworth K T, McGarry C K, Trainor C, McMahon S J, O'Sullivan J M, Schettino G, Hounsell A R and Prise K M 2012 Dose, dose-rate and field size effects on cell survival following exposure to non-uniform radiation fields *Phys. Med. Biol.* **57** 3197–206

Butterworth K T, McGarry C K, Trainor C, O'Sullivan J M, Hounsell A R and Prise K M 2011 Out-of-field cell survival following exposure to intensity-modulated radiation fields *Int. J. Radiat. Oncol. Biol. Phys.* **79** 1516–22

Ebert M, Suchowerska N, Jackson M and McKenzie D R 2010 A mathematical framework for separating the direct and bystander components of cellular radiation response *Acta Oncologica* **49** 1334–43

Engels B, Soete G, Verellen D and Storme G 2009 Conformal arc radiotherapy for prostate cancer: increased biochemical failure in patients with distended rectum on the planning computed tomogram despite image guidance by implanted markers *Int. J. Radiat. Oncol. Biol. Phys.* **74** 388–91

Heemsbergen W D, Al-Mamgani A, Witte M G, van Herk M and Lebesque J V 2013 Radiotherapy with rectangular fields is associated with fewer clinical failures than conformal fields in the high-risk prostate cancer subgroup: results from a randomized trial *Radiother. Oncol.* **107** 134–9

Herschtal A, Foroudi F, Silva L, Gill S and Kron T 2013 Calculating geometrical margins for hypofractionated radiotherapy *Phys. Med. Biol.* **58** 319–33

ICRU 1993 *Prescribing, Recording, and Reporting Photon Beam Therapy* (*ICRU Report* vol 50) (Bethesda, MD: International Commission on Radiation Units and Measurements)

King C R, Brooks J D, Gill H and Presti J C 2012 Long-term outcomes from a prospective trial of stereotactic body radiotherapy for low-risk prostate cancer *Int. J. Radiat. Oncol. Biol. Phys.* **82** 877–82

Loblaw A *et al* 2013 Prostate stereotactic ablative body radiotherapy using a standard linear accelerator: toxicity, biochemical, and pathological outcomes *Radiother. Oncol.* **107** 153–8

Mackonis E C, Suchowerska N, Zhang M, Ebert M, McKenzie D R and Jackson M 2007 Cellular response to modulated radiation fields *Phys. Med. Biol.* **52** 5469–82

Malmström A *et al* 2012 Temozolomide versus standard 6-week radiotherapy versus hypofractionated radiotherapy in patients older than 60 years with glioblastoma: the Nordic randomised, phase 3 trial *Lancet Oncol.* **13** 916–26

Mancuso M, Giardullo P, Leonardi S, Pasquali E, Casciati A, De Stefano I, Tanori M, Pazzaglia S and Saran A 2013 Dose and spatial effects in long-distance radiation signaling *in vivo*: implications for abscopal tumorigenesis *Int. J. Radiat. Oncol. Biol. Phys.* **85** 813–9

Mancuso M *et al* 2008 Oncogenic bystander radiation effects in *Patched* heterozygous mouse cerebellum *Proc. Natl Acad. Sci.* **105** 12445–50

McBride S M, Wong D S, Dombrowski J J, Harkins B, Tapella P, Hanscom H N, Collins S P and Kaplan I D 2012 Hypofractionated stereotactic body radiotherapy in low-risk prostate adenocarcinoma: preliminary results of a multi-institutional phase 1 feasibility trial *Cancer* **118** 3681–90

McGarry C K, Butterworth K T, Trainor C, McMahon S J, O'Sullivan J M, Prise K M and Hounsell A R 2012 *In-vitro* investigation of out-of-field cell survival following the delivery of conformal, intensity-modulated radiation therapy (IMRT) and volumetric modulated arc therapy (VMAT) plans *Phys. Med. Biol.* **57** 6635–45

McMahon S J, Butterworth K T, Trainor C, McGarry C M, O'Sullivan J M, Schettino G, Hounsell A R and Prise K M 2013 A kinetic-based model of radiation-induced intercellular signalling *PLoS ONE* **8** e54526

McMahon S J, Butterworth K T, McGarry C K, Trainor C, O'Sullivan J M, Hounsell A R and Prise K M 2012 A computational model of cellular response to modulated radiation fields *Int. J. Radiat. Oncol. Biol. Phys.* **84** 250–6

McMahon S J, McGarry C K, Butterworth K T, O'Sullivan J M, Hounsell A R and Prise K M 2013 Implications of intercellular signaling for radiation therapy: a theoretical dose-planning study *Int. J. Radiat. Oncol. Biol. Phys.* **87** 1148–54

Onishi H *et al* 2004 Stereotactic hypofractionated high-dose irradiation for stage I nonsmall cell lung carcinoma: clinical outcomes in 245 subjects in a Japanese multiinstitutional study *Cancer* **101** 1623–31

Partridge M 2008 A radiation damage repair model for normal tissues *Phys. Med. Biol.* **53** 3595–608

Prise K M and O'Sullivan J M 2009 Radiation-induced bystander signalling in cancer therapy *Nat. Rev. Cancer* **9** 351–60

Selvaraj J, Uzan J, Baker C and Nahum A 2013 Loss of local control due to tumor displacement as a function of margin size, dose-response slope, and number of fractions *Med. Phys.* **40** 041715

Sheu T, Molkentine J, Transtrum M K, Buchholz T A, Withers H R, Thames H D and Mason K A 2013 Use of the LQ model with large fraction sizes results in underestimation of isoeffect doses *Radiother. Oncol.* **109** 21–5

Suchowerska N, Ebert M A, Zhang M and Jackson M 2005 *In vitro* response of tumour cells to non-uniform irradiation *Phys. Med. Biol.* **50** 3041–51

Tree A C, Khoo V S, van As N J and Partridge M 2014 Is biochemical relapse-free survival after profoundly hypofractionated radiotherapy consistent with current radiobiological models? *Clin. Oncol.* **26** 216–29

Van Herk M, Remeijer P, Rasch C and Lebesque J V 2000 The probability of correct target dosage: dose-population histograms for deriving treatment margins in radiotherapy *Int. J. Radiat. Oncol. Biol. Phys.* **47** 1121–35

van Herk M 2004 Errors and margins in radiotherapy *Semin. Radiat. Oncol.* **14** 52–64

Verhaegen F, Granton P and Tryggestad E 2011 Small animal radiotherapy research platforms *Phys. Med. Biol.* **56** 55–83